ASSESSMENT OF ABUNDANCE OF Mg-SPINEL USING M³ DATA: THE THEOPHILUS CRATER PEAK. Y. Surkov[1], V. Kaydash[2], Y. Shkuratov[2], G. Videen[3], U. Mall[1]; [1]Max Planck Institute for Solar System Research, Justus-von-Liebig-Weg 3, Göttingen 37077, Germany. [2]Inst. Astron., V. N. Karazin Kharkiv Nat. Univ., 35 Sumska Str., Kharkiv, 61022, Ukraine. [3]Space Sci. Inst., 4765 Walnut St, Suite B Boulder, CO 80301, USA.

Introduction: Mg-spinel has been found on the lunar surface from the Apollo sample collections and the Chandrayaan-1 M³ spectral measurements [1,2]. Mg-spinel sites are compact (hundred meters of length) areas occurring widespread over the Moon's surface on the crater's central peaks, rims, and mounts around the mares [3]. Some data show spinel in pyroclastic deposits [4,5]. Spectral studying of Mg-spinel deposits revealed that they are associated with pink spinel anorthosites [3]. The geological analysis of collected data allowed several models of Mg-spinel formation on the Moon [e.g. 6-9]. Spectral detection of spinels is usually based on visual inspection of the absorption band near 2 μm. We aim here to present a simple technique to identify and map Mg-spinel robustly using M³ data.

Studied region and source data: We chose the region of the central peak of the Theophilus crater 11.4°S 26.4°E (Fig. 1, left). This peak is a spectrally confirmed site of Mg-spinel deposits [e.g. 3,10,11]. Dhingra et al. [10] found multiple Mg-spinel deposits, crystalline plagioclase areas across the region and also pointed on the lack of any mafic (Fe-bearing) minerals on the peak material. However, the pyroxene spectral signatures are present on the crater floor and walls; thus, they cannot be completely excluded from the analysis. Modeling mineral abundances performed by Lemelin et al. [12] also show olivine abundance (up to 10 wt.%) on the northeast massif of the peak. Lal et al. [11] suggested that the deposits enriched with Mg-spinel were rather produced by the Theophilus crater formation than during later secondary events.

To study this region, we used a portion of M³ hyperspectral image M3G20090731T045352. We applied the data processing procedure described in [13,14]. This allows one to suppress the artifact pattern of long narrow vertical stripes on the reflectance image preserving the spectral and spatial resolutions.

Spinel identification and abundance assessment: Our idea is to utilize multivariable linear regression for Mg-spinel remote sensing. Such approaches have been used to estimate and map the abundances of plagioclase, pyroxenes and agglutinates, as well as OMAT index [e.g. 15,16]. We proposed the following expression:

$$W[\text{wt.\%}] = a_1 + a_2 C(0.95/0.75\ \mu m) + a_3 C(2.65/1.55\ \mu m)$$

We used two color ratios, C(0.95/0.75 μm) and C(2.65/1.55 μm), which are the ratios of spectral albedo at corresponding wavelengths and free coefficients a_1, a_2, and a_3 that should be fitted. This formula has a clear spectroscopic meaning: the spinel-bearing deposits might have a high value of C(0.95/0.75 μm) as they are associated with the lack of Fe-bearing minerals, but at the same time the values of C(2.65/1.55 μm) should be low as the spinel has an absorption band at 2.65 μm.

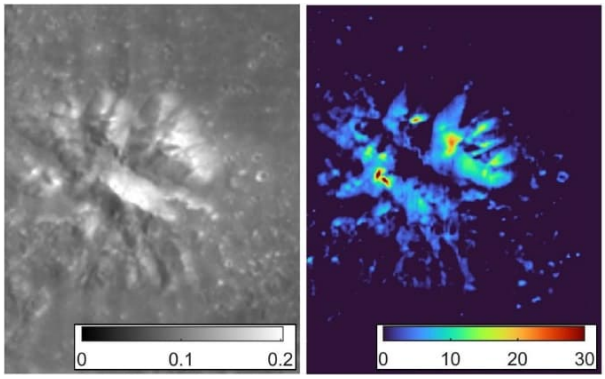

Figure 1. The reflectance image (left) and spinel abundance distribution in wt.% (right).

The standard procedure of the free coefficients estimate assumes fitting the expression using laboratory spectra and compositional analysis of lunar samples, e.g., from the LSCC database. However, we used another possibility. We constructed a set of 10,000 synthetic spectra using the 1D spectral-mixing model [17]. These spectra and model concentrations were calculated for the mixtures of five minerals in arbitrary proportions: plagioclase (PLG), spinel (SPL), olivine (OLV), pyroxenes (PYR) and a material extremely affected by space weathering – agglutinates (AGL).

The structural parameters of this model are the free path of light in regolith (taken as 20 μm) and the volume fraction occupied by particles (equal to 0.5). The refractive indices of minerals are n_{plg} = 1.5; n_{spl} = 1.7; n_{olv} = 1.6; n_{pyr} = 1.6; n_{agl} = 2. To calculate the absorption spectra of minerals we used the spectra from the LRMCC dataset [18] for the fine fractions of PLG –LRCMP210_15058; PYR – LRCMP213_15555; OLV– LRCMP212_15555. Spinel spectrum is SP117 from [19]. The spectrum of AGL is LS-CMP-045 from the RELAB database. To model the spectral effects of $npFe^0$ granules, the Maxwell-Garnet effective media theory was applied, modifying the spectra of the absorption coefficients of pure minerals. The $npFe^0$ volume fraction was distributed from 0 to $5 \cdot 10^{-4}$. The model uses the volume concentration of each mineral

c_m, so we estimated the weighted per cents of spinel as W_{spl} [wt.%] = $\rho_{spl} c_{spl} / \Sigma_{m=1..5} \rho_m c_m$, where ρ_m is the density: ρ_{plg} = 2.65 g·cm^{-3}; ρ_{spl} = 3.6 g·cm^{-3}; ρ_{olv} = 3.3 g·cm^{-3}; ρ_{pyr} = 3.4 g·cm^{-3}; ρ_{agl} = 3.4 g·cm^{-3}.

Finally, performing the fitting of free coefficients using our spectral dataset, the following values of free parameters were obtained: a_1 = 86.75; a_2 =14.25 and a_3 =-75.5. Note that linear models can produce negative values of W_{spl} that is physical nonsense. This case should be interpreted as the absence of spinel.

Results and discussion: The results of spinel abundance mapping are shown in the right panel of Fig. 1. The average abundance of spinel is 6.5 wt. % (excluding the area without identified spinel); however, this mineral varies widely over the peak surface. We can conditionally divide spinel areas into three types: (1) tops of peaks, (2) peak slopes, and (3) floor deposits. The major tops of the peak show the highest spinel abundance. The composition of the central peak is considered to be composed of materials from the interior, which are metamorphosized by temperature and pressure during the uplifting by the impact process. Thus, the estimated spinel distribution supports the hypothesis of the origin of Mg-spinel as excavated materials of the Mg-reach pluton or parts of the lunar Mg-suit proposed by Lal et al. [11].

Several sites were identified on the high-resolution NAC data (Fig. 2). While the main Mg-spinel deposits are located on the tops and ridges of the crater peak massif, other spinel abundant sites are the falls of boulders from steep mountain slopes that involve the shifting of the regolith as well. Minor spinel exposures scattered around the crater mostly are not coincident with craters. The main common characteristic of all spinel deposits is their affinity with the visually bright spots with jagged diffuse edges. The size of the areas varies from tens of meters to a few kilometers. Several examples of them are presented on the portions of NAC images on Fig. 2. Besides higher albedo, all these areas also have massive piles of stones and boulders of various sizes from several to ten meters.

The area (1) is the spur between two main parts of the peak (see Fig. 2). The spinel spectral signature is identified strictly by the slope covered with boulders. The area (2) shows two distant craters: one has a visually smooth area and the other has complicated surface morphology of the inner part covered with boulders. The distinct spinel spectral feature is seen on the second crater, albeit its diameter is only about twice more than the M^3 spatial resolution. The areas (3) and (4) represent the small spinel exposures on one of the minor tops and near the foot of the Theophilus peak, respectively. We presented these areas here to show that these observed effects cannot be due to the complicated topography as they are located on the relatively horizontal surface. Further analysis of the origin of these fields of boulders may shed light on the origin of Mg-spinel surface exposures themselves.

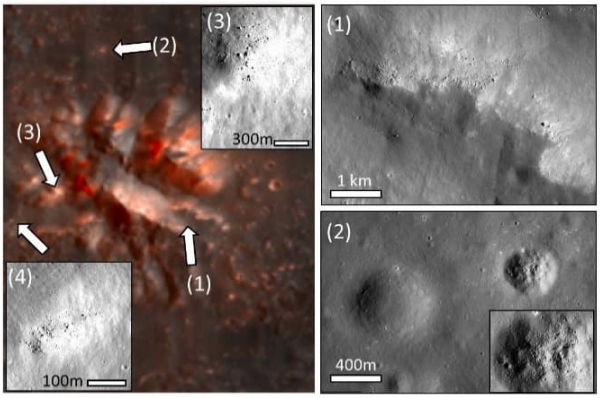

Figure 2. High-resolution studying of spinel deposits. NAC images are from https://quickmap.lroc.asu.edu/

Conclusions: We presented an approach to identify and assess the abundance of Mg-spinel using the linear combination of color ratios C(0.95/0.75μm) and C(2.65/1.55μm), which we applied to M^3 data for the central peak of Theophilus crater. Our results are in good agreement with previous studies of this region [10,11]. The Mg-spinel content in the area varies significantly. The regolith of the main massif contains from 3-4 to 10 wt.%; whereas several small sites on tops and along mountain ridges show higher values. The spectral analysis reveals that the spinel can manifest itself by producing a clear absorption feature at 2 μm, as well as the lowering of the spectral slope after 1.5 μm, if the abundance is less than 10 wt.%. This can be important for further investigations of Mg-spinel surface exposures over the Moon's surface.

References: [1] Roedder E. and Weiblen P. (1972) *Earth & Planet. Sci. Lett.15(4),* 376-402. [2] Pieters C. et al. (2011) *JGR 116,* E00G08. [3] Pieters C. et al. (2014) *Amer. Mineral. 99,* 1893-1910. [4] Sunshine J. et al. (2014) *LPSC 45th,* 2295. [5] Yamamoto S. et al. (2013) *JGR 40,* 4549-45554. [6] Weitz C. et al. (2017) *JGR: Planets 122,* 2013-2033. [7] Gross J. and Treiman A. (2011) *JGR 116,* E10009. [8] Taylor L. and Pieters C. (2013) *Icarus 233,* 749-765. [9] Prissel T. et al. (2014) *Earth & Planet. Sci. Lett. 403,* 144-156. [10] Dhingra D. et al. (2011) *Geophys. Res. Lett. 38,* L11201. [11] Lal D. et al. (2012) *J. Earth Syst. Sci. 121(3),* 847-853. [12] Lemelin M. et al. (2019) *PSS 165,* 230-243. [13] Shkuratov Y. et al. (2019) *Icarus 321,* 34-49. [14] Surkov Y. et al. (2020) *Icarus 341,* 113661. [15] Pieters C. et al. (2002) *Icarus 155,* 285-298. [16] Shkuratov Y. et al. (2005) *Sol. Syst. Res. 39(4),* 255-266. [17] Shkuratov Y. et al. (2011) *Planet. Space Sci. 59,* 1326-1371. [18] Isaacson P. et al. (2011) *Meteorit. Planet. Sci. 46,* 228-251. [19] Cloutis E. et al. (2004) *Meteorit. Planet. Sci. 39,* 545-565.